Contribution from the Department of Chemistry,
The University of Houston—University Park, Houston, Texas 77004

A Reinvestigation of Silver Porphyrin Electrochemistry. Reactions of Ag(III), Ag(II), and Ag(I)

K. M. Kadish,* X. Q. Lin, J. Q. Ding, Y. T. Wu, and C. Araullo

Received February 25, 1986

The homogeneous and heterogeneous oxidation and reduction of silver porphyrins were investigated in nonaqueous media. Eleven complexes of ((*p*-X)TPP)Ag (where TPP = the dianion of tetraphenylporphyrin) were electrochemically investigated in CH_2Cl_2, Me_2SO, and pyridine. Up to four reversible electrode reactions were observed for each complex. These corresponded to the formation of Ag(III), Ag(III) cation radicals, Ag(I), and Ag(I) anion radicals. No evidence of demetalation was observed on the spectroelectrochemical time scale, and reversibly generated spectra of the Ag(I) complexes were obtained. Surprisingly, these spectra resembled those of $(TPP)Ag_2$. The oxidation of ((*p*-X)TPP)Ag by Ce(IV) and the reduction of ((*p*-X)TPP)Ag by N_2H_4 were also investigated. The former reaction generated $[((p\text{-X})TPP)Ag^{III}]^+$ while the latter generated Ag^0 and $(TPP)H_2$. Rate constants were calculated for the chemical oxidation of Ag(II) to Ag(III) as well as the demetalation of Ag(II) or Ag(I) by N_2H_4. Correlations were made between these chemical rate constants and the sum of the substituent constants, 4σ, for ((*p*-X)TPP)Ag. Correlations were also made between the spectral and electrochemical properties of ((*p*-X)TPP)Ag. In addition, linear free energy relationships involving electrochemical data and electronic absorption spectra are reported.

Introduction

A number of papers have reported the electrochemical reactivity of Ag(II) porphyrins.[1-15] Air-stable silver porphyrin complexes contain Ag(II), but the oxidation of Ag(II) to Ag(III) can occur under either chemical or electrochemical conditions. An additional oxidation of the Ag(III) complex and/or reduction of the Ag(II) porphyrin is also possible, but very little is known about these reactions. In addition, the data in the literature are not internally self-consistent. For example, the electrochemical reduction of (OEP)Ag in Me_2SO (where OEP = the dianion of octaethylporphyrin) was initially reported to involve the porphyrin π-ring system,[3] but later more detailed studies of (OEP)Ag and (TPP)Ag in DMF, pyridine, and CH_2Cl_2 (where TPP = the dianion of tetraphenylporphyrin) showed that reduction of the complex involved formation of Ag(I) followed by a demetalation.[12,13]

Information is also not available as to how changes in solvent affect the oxidation of Ag(III) porphyrins. Only two reports of Ag(III) porphyrin oxidation have been published,[5,11] but the results of these two studies are not internally self-consistent. Jones and Po[11] reported that $[(TPP)Ag^{III}]^+$ was oxidized to $[(TPP)Ag^{III}]^{2+}$ at +1.34 V vs. SCE in CH_2Cl_2 while Antipas et al.[5] gave an $E_{1/2}$ of +1.64 V vs. SCE for this reason in the same solvent system. Data in other solvent systems have not been reported.

In this paper we have used cyclic voltammetry and thin-layer spectroelectrochemistry to investigate the electrode reactions of Ag(III), Ag(II), and Ag(I) porphyrins. These reactions were investigated in CH_2Cl_2, Me_2SO, and pyridine and are given by eq 1-4 where (*p*-X)TPP is one of 11 different para-substituted

$$((p\text{-X})TPP)Ag^{II} \rightleftarrows [((p\text{-X})TPP)Ag^{III}]^+ + e^- \quad (1)$$

$$[((p\text{-X})TPP)Ag^{III}]^+ \rightleftarrows [((p\text{-X})TPP)Ag^{III}]^{2+} + e^- \quad (2)$$

$$((p\text{-X})TPP)Ag^{II} + e^- \rightleftarrows [((p\text{-X})TPP)Ag^{I}]^- \quad (3)$$

$$[((p\text{-X})TPP)Ag^{I}]^- + e^- \rightleftarrows [((p\text{-X})TPP)Ag^{I}]^{2-} \quad (4)$$

tetraphenylporphyrin derivatives. Complexation of solvent molecules or counterions from the supporting electrolyte may occur, but for simplicity these reactions are not indicated in eq 1-4.

Spectra for electrogenerated $[((p\text{-X})TPP)Ag^{III}]^{2+}$, $[((p\text{-X})TPP)Ag^{III}]^+$, $[((p\text{-X})TPP)Ag^{I}]^-$, and $[((p\text{-X})TPP)Ag^{I}]^{2-}$ are presented for the first time, and a detailed electrochemical study of substituent effects is presented for reactions 1-4. We have also utilized the stopped-flow technique to study substituent effects on rate constants for the homogeneous oxidation of ((*p*-X)TPP)Ag^{II} with Ce(IV) in Me_2SO. Similar experiments were carried out for the chemical reduction of ((*p*-X)TPP)Ag^{II} by N_2H_4, but a demetalation to generate Ag^0 and ((*p*-X)TPP)H_2 was observed.

Experimental Section

Instrumentation. Cyclic voltammetric measurements were obtained with a PAR Model 174 polarographic analyzer. A three-electrode system was used for conventional cyclic voltammetry. This consisted of a 0.8-mm^2 platinum-button working electrode, an aqueous saturated calomel reference elecltrode (SCE), and a platinum-wire auxiliary electrode. The vacuum-tight thin-layer spectroelectrochemical cell contained a doublet platinum-gauze working electrode and has been described in the literature.[16] A Tracor Northern TN-1710 rapid-scanning spectrometer was used for obtaining thin-layer spectra. A dual-beam IBM Model 9430 UV-visible spectrophotometer was used for recording spectra of the neutral complexes. Stopped-flow measurements were obtained with a Durrum D103 stopped-flow system that was combined with the Tracor Northern TN-1710 multichannel analyzer to obtain time-resolved spectra. A Hewlett Packard 3310 B function generator was used to control the spectral acquisitions.

Materials. Synthesis of ((*p*-X)TPP)Ag^{II} was according to procedures described in the literature.[17,18] Tetrabutylammonium perchlorate (TBAP) (Fluka Chemical Co.) was used as supporting electrolyte in the electrochemical measurements. This salt was recrystallized from ethanol and dried in vacuo before use. Analytical grade dichloromethane (CH_2Cl_2) (J. T. Baker Chemical Co.) was freshly distilled from P_2O_5 before use. Dimethyl sulfoxide (Me_2SO) (Aldrich Chemical Co.) and pyridine (py) (Fisher Scientific Co.) were freshly distilled under reduced pressure.

(1) Stanienda, A.; Biebl, G. *Z. Phys. Chem. (Munich)* **1967**, *52*, 254.
(2) Kadish, K. M.; Davis, D. G.; Fuhrhop, J. H. *Angew. Chem., Int. Ed. Engl.* **1972**, *11*, 1014.
(3) Fuhrhop, J.-H.; Kadish, K. M.; Davis, D. G. *J. Am. Chem. Soc.* **1973**, *95*, 5140.
(4) Karweik, D.; Winograd, N.; Davis, D. G.; Kadish, K. M. *J. Am. Chem. Soc.* **1974**, *96*, 591.
(5) Antipas, A.; Dolphin, D.; Gouterman, M.; Johnson, E. C. *J. Am. Chem. Soc.* **1978**, *100*, 7705.
(6) Kadish, K. M.; Morrison, M. M. *Bioinorg. Chem.* **1977**, *7*, 107.
(7) Krishnamurthy, M. *Inorg. Chem.* **1978**, *17*, 2242.
(8) Giraudeau, A.; Gallot, H. J.; Jordan, J.; Ezhar, I.; Gross, M. *J. Am. Chem. Soc.* **1979**, *101*, 3857.
(9) Giraudeau, A.; Callot, H. J.; Gross, M. *Inorg. Chem.* **1979**, *18*, 201.
(10) Morano, D. J.; Po, H. N. *Inorg. Chim. Acta* **1978**, *31*, L421.
(11) Jones, S. E.; Po, H. N. *Inorg. Chim. Acta* **1980**, *42*, 95.
(12) Giraudeau, A.; Louati, A.; Callot, H. J.; Gross, M. *Inorg. Chem.* **1981**, *20*, 769.
(13) Kumar, A.; Neta, P. *J. Phys. Chem.* **1981**, *85*, 2830.
(14) Po, H. N.; Jones, S. E. *Inorg. Chim. Acta* **1981**, *48*, 37.
(15) Po, H. N. *Coord. Chem. Rev.* **1976**, *20*, 171.
(16) Lin, X. Q.; Kadish, K. M. *Anal. Chem.* **1985**, *57*, 1498.
(17) Adler, A. D.; Longo, F. R.; Finarelli, J. D.; Goldmacher, J.; Assour, J.; Korsakoff, L. *J. Org. Chem.* **1967**, *32*, 476.
(18) Eaton, S. S.; Eaton, G. R. *J. Am. Chem. Soc.* **1975**, *97*, 3660.

0020-1669/86/1325-3236$01.50/0

Table I. Half-Wave Potentials (V vs. SCE) for the Oxidation and Reduction of ((*p*-X)TPP)Ag^{II} in CH_2Cl_2, 0.1 M TBAP

porphyrin	2nd oxidn	1st oxidn	1st redn	2nd redn	4σ[a]
((*p*-NO_2)TPP)Ag	1.74	0.78	−0.83		3.12
((*p*-CN)TPP)Ag	1.73	0.78	−0.86	−1.43	2.64
((*p*-CF_3)TPP)Ag	1.70	0.74	−0.93		2.20[b]
((*p*-Cl)TPP)Ag	1.63	0.64	−0.96		0.92
((*p*-F)TPP)Ag	1.63	0.64	−0.99		0.24
(TPP)Ag	1.62	0.59	−1.01		0.00
((*p*-CH_3)TPP)Ag	1.57	0.53	−1.04		−0.68
((*p*-OC_2H_5)TPP)Ag	1.49	0.47	−1.07		−1.00
((*p*-OCH_3)TPP)Ag	1.53	0.49	−1.05		−1.08
((*p*-$OCH_2C_6H_5$)TPP)Ag	1.52	0.50	−1.05		−1.64
((*p*-NEt_2)TPP)Ag			−1.06		−2.80[b]

[a] Taken from ref 31. [b] Taken from ref 32.

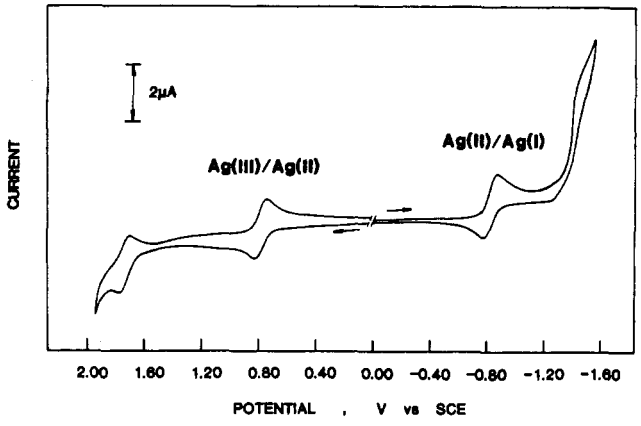

Figure 1. Cyclic voltammogram of ((*p*-CN)TPP)Ag in CH_2Cl_2, 0.1 M TBAP. Scan rate = 100 mV/s.

Reagent grade hydrazine (N_2H_4) (Fisher Scientific Co.) was used directly without further purification. All other chemicals were analytical grade.

Results and Discussion

Electrochemistry and Spectroelectrochemistry of ((*p*-X)TPP)Ag^{II}. Cyclic voltammetric characterization of each complex was carried out in CH_2Cl_2, Me_2SO, and pyridine containing 0.1 M TBAP. Half-wave potentials are listed in Tables I and II and a typical voltammogram of ((*p*-CN)TPP)Ag in CH_2Cl_2 is shown in Figure 1. Three well-defined electrode reactions are observed for this complex in CH_2Cl_2. These occur at $E_{1/2}$ = +1.73, +0.78, and −0.86 V. A fourth process can also be seen at about −1.43 V, but this reduction is superimposed on a large background current of the solvent.

The first oxidation or the first reduction of ((*p*-X)TPP)Ag occurs at similar potentials in CH_2Cl_2, py, or Me_2SO when $E_{1/2}$ values are measured vs. an SCE and are not corrected for liquid-junction potential. However, measurements of $E_{1/2}$ vs. an internal standard such as ferrocene or bis(biphenyl)chromium may lead to more significant differences in potential[19] and this type of data can be used to indicate the type and degree of solvent–solute interaction.[20]

Comparisons between half-wave potentials for the second oxidation or for the second reduction of ((*p*-X)TPP)Ag in CH_2Cl_2, Me_2SO, and py are not possible due to the fact that the three utilized solvents do not have similar large positive and negative potential windows. The potential window of pyridine and Me_2SO extends to about −2.0 and −1.8 V, respectively, and in these solvents two well-defined reductions of ((*p*-X)TPP)Ag are observed. Values of $E_{1/2}$ are given in Table II. Reversible potentials for the second reduction range between −1.43 and −1.77 V. vs. SCE in pyridine and between −1.26 and −1.50 V vs. SCE in Me_2SO. In addition, each ((*p*-X)TPP)Ag complex exhibited a prewave in Me_2SO. Potentials for this prewave varied between −0.7 and −0.8 V depending upon the specific complex. A similar prewave has been reported for the reduction of other (TPP)M complexes in the same solvent system.[21]

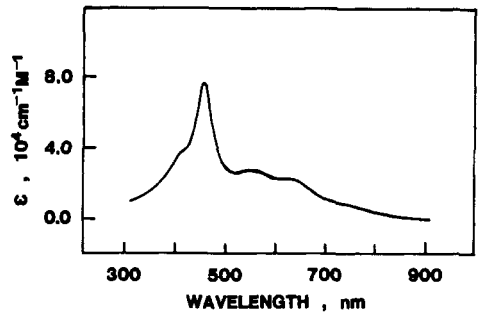

Figure 2. Spectrum of the species generated from ((*p*-OC_2H_5)TPP)Ag by oxidation at +1.6 V in CH_2Cl_2, 0.1 M TBAP.

The first oxidation of ((*p*-X)TPP)Ag involves the Ag(II)/Ag(III) transition,[2,5,11] and this reaction occurs at 0.78 V for ((*p*-CN)TPP)Ag in CH_2Cl_2. The second oxidation of ((*p*-CN)TPP)Ag as well as those of the other ((*p*-X)TPP)Ag complexes can be assigned as abstraction of an electron from the porphyrin π ring. Evidence for this assignment comes in part from thin-layer spectra taken before and after electrooxidation of the Ag(III) complex. A spectrum of the final product after the abstraction of two electrons from ((*p*-OC_2H_5)TPP)Ag at +1.6 V in CH_2Cl_2 is shown in Figure 2 and provides one example. The product of the two-electron oxidation has broad absorption bands that cover a range of wavelengths from 300 to 800 nm. This spectrum can be clearly characterized as that of a π cation radical.[22,23]

Giraudeau et al.[12] reported that (TPP)Ag^{II} is reduced at a mercury electrode in three one-electron steps that occur at −0.88, −1.65, and −2.01 V vs. SCE in DMF containing 0.1 M tetra-*n*-hexylammonium perchlorate (THAP). According to molecular orbital energy diagrams, Ag(I) should be formed in the first reduction,[5] and this was experimentally observed.[12] However, electrochemical studies in DMF showed that demetalation occurred after Ag(I) formation. This is not the case in CH_2Cl_2, as demonstrated by the well-defined reduction illustrated in Figure 1. Also, the second and third reductions reported by Giraudeau et al.[12] corresponded to reactions of generated $(TPP)H_2$. In the present study, minimal amounts of $(TPP)H_2$ were formed on the cyclic voltammetric time scale and the reduction peaks in Figure 1 correspond to the reversible reactions given by eq 3 and 4.

Potential differences between the first ring oxidation and the first ring reduction of numerous octaethyl- and tetraphenylporphyrins can generally be related to the energy difference between the HOMO and LUMO of the porphyrin π-ring system[24] and has been determined to be in the range of 2.25 ± 0.15 V.[2,3] However, a number of exceptions have been found to this general rule. These exceptions include metalloporphyrins containing Fe, Co, Mn, and Mo. The complexes of ((*p*-X)TPP)Ag also present an exception to this rule. The generation of a ((*p*-CN)TPP)Ag^{III} π cation radical (reaction 2) occurs at +1.73 V so that the generation of a π anion radical would be expected to occur at about −0.52 V if the general rule were applied. The first reduction of ((*p*-CN)TPP)Ag occurs at −0.86 V but this reaction involves

(19) Values of $E_{1/2}$ vs. an internal reference couple such as the ferrocene/ferrocenium couple or the bis(biphenyl)chromium(O/I) couple will eliminate differences in liquid-junction potential between different nonaqueous solvents and will provide potentials that indicate real thermodynamic differences in solvent–solute interactions between two different nonaqueous solvents. This is discussed by Kadish and Gritzner for the reduction of tetraphenylporphyrin complexes with seven different central metal ions in fourteen different nonaqueous solvent systems.[20]

(20) Kadish, K. M.; Cornillon, J.-L.; Yao, C. L.; Malinski, T.; Gritzner, G., submitted for publication.

(21) Felton, R.; Linschitz, J. *J. Am. Chem. Soc.* **1966**, *88*, 1113.
(22) Wolberg, A.; Manassen, J. *J. Am. Chem. Soc.* **1970**, *92*, 2982.
(23) Fuhrhop, J.-H. *Struct. Bonding (Berlin)* **1974**, *18*, 1–68.
(24) Zerner, M.; Gouterman, M. *Theor. Chim. Acta* **1967**, *8*, 26.

Table II. Half-Wave Potentials (V vs. SCE) for the Oxidation and Reduction of ((*p*-X)TPP)Ag^{II} in Me_2SO and Pyridine Containing 0.1 M TBAP

	Me_2SO			pyridine			
porphyrin	oxidn	1st redn[a]	2nd redn	oxidn	1st redn	2nd redn	4σ[b]
((*p*-NO_2)TPP)Ag	0.68			0.75			3.12
((*p*-CN)TPP)Ag	0.70	−0.80	−1.26	0.73	−0.78	−1.43	2.64
((*p*-CF_3)TPP)Ag	0.66	−0.80		0.71	−0.85	−1.49	2.20
((*p*-Cl)TPP)Ag	0.62	−0.91	−1.31	0.64	−0.90	−1.60	0.92
((*p*-F)TPP)Ag	0.59	−0.92		0.61	−0.90	−1.61	0.24
(TPP)Ag	0.58	−1.03		0.58	−0.96	−1.67	0.00
((*p*-CH_3)TPP)Ag	0.53	−1.00	−1.40	0.53	−0.98	−1.70	−0.68
((*p*-OC_2H_5)TPP)Ag	0.53	−1.01	−1.40	0.48	−0.98	−1.71	−1.00
((*p*-OCH_3)TPP)Ag	0.51	−1.02	−1.44	0.50	−0.98	−1.72	−1.08
((*p*-$OCH_2C_6H_5$)TPP)Ag	0.54	−1.00		0.49	−0.98	−1.73	−1.64
((*p*-NEt_2)TPP)Ag	0.38	−1.08	−1.50	0.32	−1.02	−1.77	−2.80[c]

[a] A prepeak was observed at potentials between −0.7 and −0.8 V depending upon the specific porphyrin. Similar prepeaks have been reported for the reduction of other (TPP)M complexes in Me_2SO.[21] [b] Taken from ref 31. [c] Taken from ref 32.

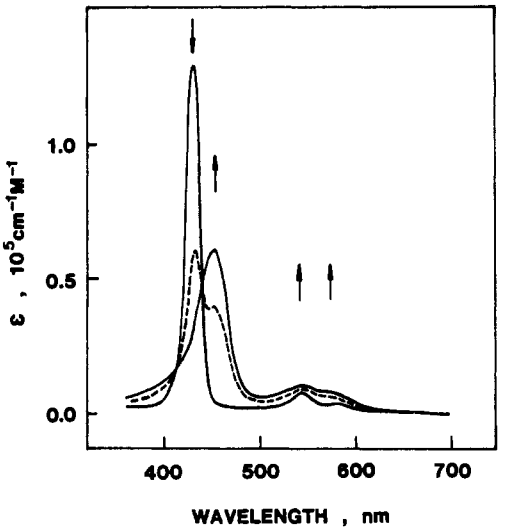

Figure 3. Potential resolved thin-layer spectral changes during the first oxidation of ((*p*-OC_2H_5)TPP)Ag in Me_2SO, 0.1 M TBAP. Potential range = 0.20–0.78 V. Scan rate = 1 mV/s.

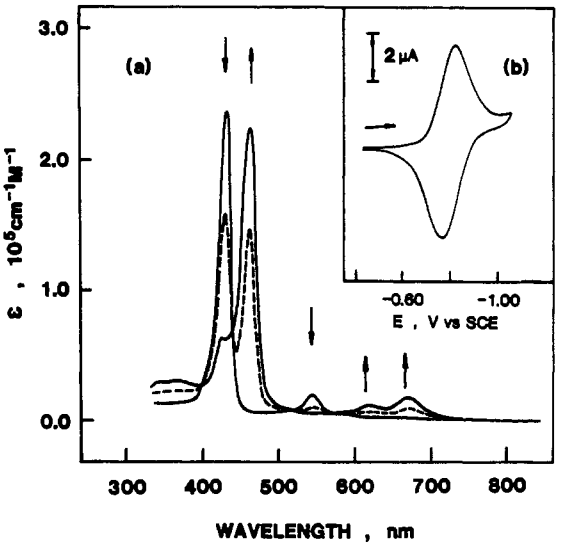

Figure 4. (a) Potential resolved thin-layer spectral changes of (TPP)Ag during the first reduction in Me_2SO, 0.1 M TBAP. Potential range = −0.60 to −1.28 V. Scan rate = 2 mV/s. (b) Corresponding thin-layer cyclic voltammogram.

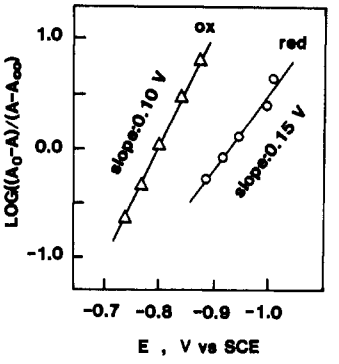

Figure 5. Analysis of the spectral data shown in Figure 4. The $(A_0 - A)/(A - A_\infty)$ ratio was determined at 422 nm as a function of potential. A_0 and A_∞ represent the absorption of (TPP)Ag and [(TPP)Ag]$^-$, respectively. Data points: (○) reduction; (△) reoxidation. (See insert of Figure 4.)

Ag(II)/Ag(I). Thus, generation of a Ag(I) π anion radical occurs at −1.43 V (see following discussions) and the absolute potential difference between the first ring oxidation and the first ring reduction of ((*p*-CN)TPP)Ag is 3.17 V. This is 0.92 V larger than for the general case.

Silver(II) has been suggested to be more covalently bonded to the porphyrin ring than other metals.[25] The strong covalent σ bonding between Ag(II) and the four pyrrole nitrogens has been examined by ESR studies.[26-28] Both the in-plane π bonding between the d_{xy} orbitals and the ligand N(p_x) or N(p_y) orbitals and the out-of-plane π bonding between one metal d_π and the N(p_z) are larger for Ag than that for Cu.[5] The significant π and σ bonding between the metal and the ring could be the origin of the bias from the general rule of a 2.25 ± 0.15 V separation between potentials for formation of the porphyrin anion and porphyrin cation radical. The ring oxidation potential is a measure of the HOMO level of the Ag(III)–ring system, but the ring reduction potential is a measure of the LUMO level of the Ag(I)–ring system.

Thin-layer spectroelectrochemistry was also used to study the formation of [((*p*-X)TPP)Ag^{III}]$^+$ and [((*p*-X)TPP)Ag^I]$^-$ from ((*p*-X)TPP)Ag (reactions 1 and 3). Spectral changes were reversible for both electrooxidation and electrorereduction, and an example of spectra obtained during electrooxidation is shown in Figure 3 for ((*p*-OC_2H_5)TPP)Ag in Me_2SO, 0.1 M TBAP. As seen in this figure, the Soret band has shifted from 429 to 450 nm during oxidation while the Q-bands have remained at their original position. Two well-defined isosbestic points in the ((*p*-OC_2H_5)TPP)Ag to [((p-OC_2H_5)TPP)Ag]$^+$ transition were found at 415 and 435 nm, and the original Ag(II) spectrum could be reversibly regenerated during the return potential sweep.

(25) Falk, J. E. *Porphyrins and Metalloporphyrins*; Elsevier: Amsterdam, 1964.
(26) MacCragh, A.; Storm, C. B.; Koski, W. S. *J. Am. Chem. Soc.* **1965**, *87*, 1470.
(27) Kneubühl, F. K.; Koski, W. S.; Caughey, W. S. *J. Am. Chem. Soc.* **1961**, *83*, 1607.
(28) Brown, T. G.; Hoffman, B. M. *Mol. Phys.* **1980**, *39*, 1073.

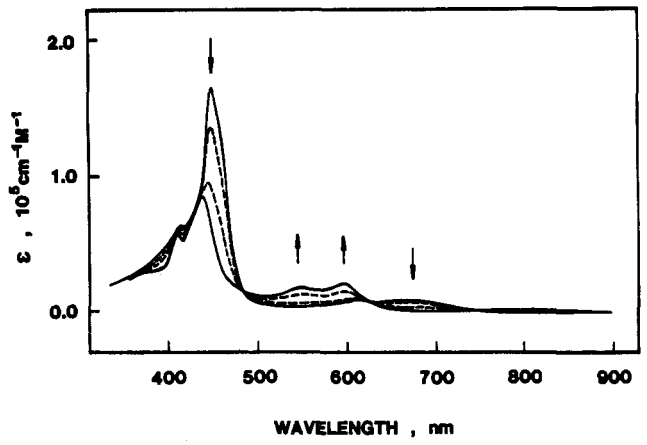

Figure 6. Potential resolved thin-layer spectral changes during the second reduction of ((*p*-OC_2H_5)TPP)Ag in py, 0.1 M TBAP. Potential range = −1.26 to −1.72 V. Scan rate = 1 mV/s.

An example of the spectral changes obtained during reduction is shown in Figure 4 for (TPP)Ag. Figure 4b shows the thin-layer cyclic voltammogram while Figure 4a shows the thin-layer spectral changes that were obtained as (TPP)Ag was reduced during a potential scan from −0.60 to −1.28 V in Me_2SO, 0.1 M TBAP. The characteristic Ag(II) absorption bands at 422 and 538 nm decreased upon reduction as three new bands appeared at 457, 616, and 667 nm. At the same time a set of well-defined isosbestic points was found at about 400, 440, 510, and 580 nm. These spectral changes were reversible, and the original Ag(II) spectrum was regenerated by a reverse potential scanning. This indicates that the electrochemical reduction of $(TPP)Ag^{II}$ is chemically reversible. However, the electrode reduction and reoxidation processes are electrochemically quasi-irreversible. This was confirmed by absorbance analysis of the spectral data, which is shwon in Figure 5. Under conditions of reversible reactions, logarithmic plots of spectral data vs. potential should be superimposable for both reductions and oxidations. On the other hand, quasi-reversible or irreversible reactions would not be superimposable and would have different apparent values of $E_{1/2}$. This is the case for (TPP)Ag, for which an example is shown in Figure 5.

The reduction of (TPP)Ag gives a linear plot of log $[(A_0 - A)/(A - A_\infty)]$ vs. potential. The slope of 0.10 V corresponds to a transfer coefficient, αn, of 0.4 and the zero intercept gives an apparent $E_{1/2}$ of −0.92. The oxidation is also characterized by a linear relationship. The slope of this plot is 0.15 V, and the apparent $E_{1/2}$ is −0.80 V. Analysis of the slope gives a value of $\beta n = 0.6$ and is thus consistent with the calculated $\alpha n = 0.4$ for reduction of the neutral complex.

Time-resolved thin-layer spectra were also obtained for (TPP)Ag as the potential was jumped from −0.60 to −1.28 V. These spectra showed the same type of changes as those illustrated in Figure 4. No intermediate spectrum was observed during reduction and the generated Ag(I) complex was quite stable under the given experimental conditions. Of most importance is that no demetalation occurred on the experimental time scale as long as the bulk solution in the thin-layer cell was well deoxygenated and the water content of Me_2SO was minimized.

Interestingly, the spectrum obtained for reduced $(TPP)Ag^{II}$ in Me_2SO (λ, nm ($\epsilon \times 10^{-4}$, cm^{-1} M^{-1}): 457 (25); 616 (1.1); 667 (1.8)) is similar to the spectrum assigned for the disilver(I) tetraphenylporphyrin in pyridine.[29] One could suggest formation of $(TPP)Ag_2$ in the present reduction process, but the formation of disilver(I) must also be accompanied by $(TPP)H_2$ formation at a molar ratio of 1:1. Free base $(TPP)H_2$ is reduced at −1.0 V to give an anion radical. However, as shown in Figure 4, neither the spectrum of neutral $(TPP)H_2$ nor that of its anion radical was found during the reduction of (TPP)Ag.

(29) Dorough, G. D.; Miller, J. R.; Hwennekens, F. M. *J. Am. Chem. Soc.* **1951**, *73*, 4315.

Table III. Homogeneous Electron-Transfer Rate Constants and Demetalation Rate Constants for ((*p*-X)TPP)Ag^{II} in Me_2SO, 0.1 M TBAP at 23 °C

porphyrin	$k_{Ag(III/II)}$, M^{-1} s^{-1} [a]	$k_{demetal}$, M^{-1} s^{-1} [b]
((*p*-CN)TPP)Ag	28	3.9×10^{-1}
((*p*-Cl)TPP)Ag	93	
(TPP)Ag	160	8.6×10^{-2}
((*p*-OC_2H_5)TPP)Ag	520	
((*p*-OCH_3)TPP)Ag	420	2.2×10^{-2}

[a] For the reaction given by eq 5. [b] For the reaction given by eq 8.

Figure 6 shows spectral changes that were monitored during the second reduction of ((*p*-OC_2H_5)TPP)Ag at $E_{1/2}$ of −1.55 V in pyridine. The initial spectrum of the complex was electrochemically generated in a thin-layer cell at −1.26 V. This spectrum shows a strong Soret band at 453 nm and Q-bands at 619 and 669 nm. These bands can thus be assigned as belonging to the $[((p\text{-}OC_2H_5)TPP)Ag]^-$ spectrum. Furthermore, increasing the applied potential to −1.72 V shows the second reduction step of this porphyrin, which is also a chemically reversible process. The Soret band decreased dramatically during the second reduction as did the band at 669 nm.

The new electrogenerated species has absorption bands at 441, 558, 603, and 837 nm, and on the basis of this spectrum the electron-transfer step can be identified as formation of a π anion radical. This reaction is given by eq 4. The spectral changes in Figure 6 were reversible, and the spectrum of Ag(II) could be regenerated with 90% recovery by reversing the potential and reoxidizing the complex at −0.35 V vs. SCE.

Kinetic Monitoring of Chemical Oxidation and Reduction. The stopped-flow technique was utilized to study the chemical oxidation of ((*p*-X)TPP)Ag by Ce(IV). The stoichiometry of the reaction between Ce(IV) and the Ag(II) porphyrins in Me_2SO was determined to be 1:1 by spectrally monitored titrations, and the final spectra were identified as those of Ag(III) porphyrins. The reaction is shown by eq 5.

$$Ce(IV) + ((p\text{-}X)TPP)Ag^{II} \xrightarrow{k_{Ag(III/II)}} Ce(III) + [((p\text{-}X)TPP)Ag^{III}]^+ \quad (5)$$

Spectral changes for oxidation of ((*p*-X)TPP)Ag^{II} were monitored as a function of time with fixed concentrations of Ce(IV). Linear relationships between the |Ln A_t| and time were found for all the selected porphyrins. Slopes of the (|Ln A_t| vs. time) plots were also linear functions of the concentration of Ce(IV). Thus, kinetics for the above oxidation can be expressed by

$$-d[((p\text{-}X)TPP)Ag^{II}]/dt = k_{Ag(III/II)}[((p\text{-}X)TPP)Ag^{II}][Ce(IV)] \quad (6)$$

Rate constants for reaction 5 were calculated for selected silver porphyrins, and these values are listed in Table III.

Stopped-flow kinetics were also used to study the reduction of ((*p*-X)TPP)Ag by hydrazine (N_2H_4 in deoxygenated Me_2SO solutions). Spectral changes after the mixing of hydrazine and ((*p*-OCH_3)TPP)Ag^{II} in a stopped-flow chamber are shown in Figure 7. After mixing, the initial spectrum converted to one that consisted of four visible absorption peaks at 524, 562, 600, and 657 nm. This spectrum is identified as that of the neutral free base porphyrin, ((*p*-OCH_3)TPP)H_2.

The demetalization of silver(I) porphyrins has been reported to occur under several different solution conditions.[7,12,13] This demetalation is attributed to the fact that the diameter of the Ag(I) ion is 1.26 Å but that for Ag(II) is only 0.89 Å. Thus an expulsion of Ag(I) from the porphyrin core may occur. In contrast, relatively stable complexes of disilver(I) have been reported.[29] The well-defined cyclic voltammogram (Figure 1) and the chemically reversible spectral changes (Figures 4 and 6) indicate that no demetalation of ((*p*-X)TPP)Ag or $[((p\text{-}X)TPP)Ag]^-$ has occurred on the time scale of the cyclic voltammetric or spectroelectrochemical experiments.

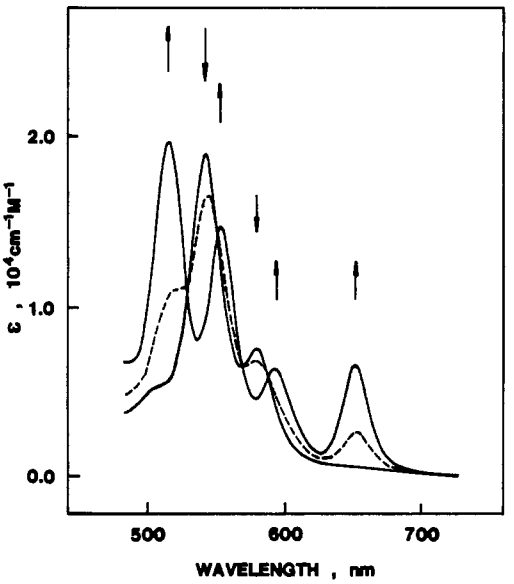

Figure 7. Spectral changes for the reaction between $((p\text{-}OCH_3)TPP)Ag^{II}$ and hydrazine in Me_2SO, 0.1 M TBAP.

Table IV. Summary of Slopes (Reaction Constants, ρ, V) from Plots of $E_{1/2}$ vs. 4σ for the Oxidation and Reduction of $((p\text{-X})TPP)Ag$ in Nonaqueous Media

	electrode reaction			
solvent	2nd oxidn	1st oxidn	1st redn	2nd redn
CH_2Cl_2	0.05	0.07	0.04	
Me_2SO		0.05	0.05	0.05
pyridine		0.07	0.04	0.07

Analysis of the stopped-flow data gave the demetalation rate equation

$$-d[((p\text{-X})TPP)Ag^{II}]/dt = k_{demetal}[N_2H_4][((p\text{-X})TPP)Ag^{II}] \quad (7)$$

and the mechanism of the demetalation reaction is thus expressed as

$$((p\text{-X})TPP)Ag^{II} + N_2H_4 \xrightarrow{k_{demetal}} Ag^0 + ((p\text{-X})TPP)H_2 + \text{products} \quad (8)$$

Evidence for the formation of $((p\text{-X})TPP)H_2$ as a product in reaction 8 comes from the spectral data (such as that presented in Figure 7) while evidence for Ag^0 formation comes from the fact that a silver coating was formed on the cell walls after several experiments. Several different products are possible from N_2H_4 oxidation,[30] but these were not characterized in the present study.

Unexpectedly, $((p\text{-X})TPP)Ag^{I}$ does not appear to be an intermediate in the chemical reduction of $((p\text{-X})TPP)Ag^{II}$. One can imagine that the homogeneous reductions of $((p\text{-X})TPP)Ag$ do not involve stable silver(I) species because hydrazine can release protons during electron transfer and these protons will accelerate the demetalation reaction.[7,13]

Rate constants for demetalation of several $((p\text{-X})TPP)Ag$ complexes were calculated, and these values are listed in Table III. It can be seen that complexes with more strongly electron-withdrawing substituents have higher demetalation rate constants. This suggests that the electron-transfer process between silver(II) and hydrazine should be the rate-determining step in these demetalation processes.

Substituent Effects, Electron-Transfer Reactions, and Electronic Absorption Spectra. Detailed studies on substituent effects for reactions 1–4 were also carried out in this study. Half-wave potentials for each of the 11 different $((p\text{-X})TPP)Ag$ complexes in CH_2Cl_2, Me_2SO, and pyridine are listed in Tables I and II, and Hammett plots of $E_{1/2}$ vs. 4σ are shown in Figure 8. Table IV lists the reaction constants calculated from plots of $E_{1/2}$ vs. 4σ in each of the three solvents. Values of σ were chosen from Jaffe and Zuman.[31,32] The electrochemical data reported by Jones and Po[11] and Antipas et al.[5] are also shown in this figure for a comparison with our data. It can be seen that the present set of data agrees well with that reported by Antipas et al.[5] The data are also in agreement with those reported by Jones and Po[11] for the first oxidation but deviate substantially from their results for the second oxidation in CH_2Cl_2.

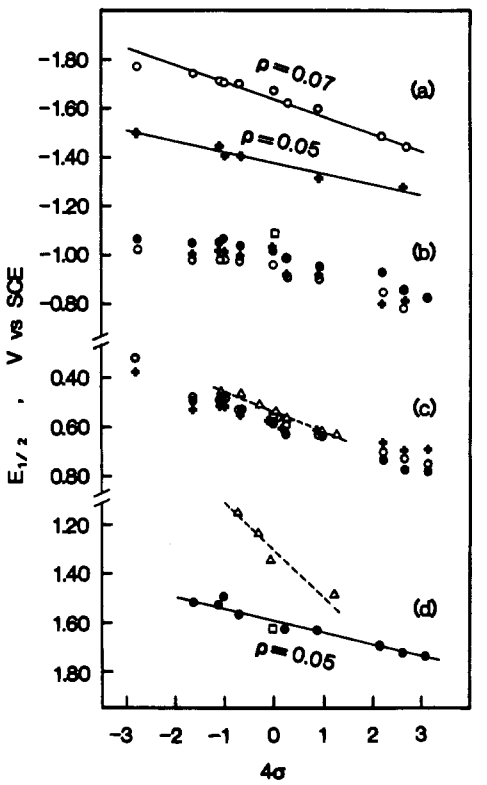

Figure 8. Linear free energy relationships between $E_{1/2}$ and 4σ for the oxidation and reduction of $((p\text{-X})TPP)Ag$ in CH_2Cl_2, Me_2SO, and py, 0.1 M TBAP: data from this study in CH_2Cl_2 (●), Me_2SO (+), and py (○); data from ref 11 (△) and ref 5 (□) in CH_2Cl_2.

Numerous substituent effects on numerous metalloporphyrin electrode reactions have been reported.[6,8,33-37] The average value of the reaction constant, ρ, for a π-ring oxidation or reduction is usually in the range of 0.070 ± 0.016.[36,37] In addition, ρ for the ring-centered reaction is usually larger than that for a metal-centered oxidation or reduction reaction.[36,37] However, as seen in Figure 8 and Table IV, the same value of ρ (0.05 ± 0.01 V) is obtained for the ring- and metal-centered reactions of $((p\text{-X})TPP)Ag$ in Me_2SO. This can be rationalized by the fact that the Ag metal ion center has significant covalent σ- and π-bonding interactions with the porphyrin ring. Because of this, partial charge transfer between the porphyrin π-ring system and metal center occurs, and this "averages out" the specific characteristics that differentiate a ring-centered reaction from a metal-centered reaction.

The slopes of $E_{1/2}$ vs. 4σ are slightly different in CH_2Cl_2 and pyridine. Values of the reaction constants, ρ, were calculated as

(30) Schmidt, E. W. *Hydrazine and Its Derivatives. Preparation, Properties, Applications*; Wiley: New York, 1984.
(31) Jaffe, H. H. *Chem. Rev.* **1953**, *53*, 191.
(32) Zuman, P. *Substituent Effects in Organic Polarography*; Plenum: New York, 1967.
(33) Malinski, T.; Chang, D.; Bottomley, L. A.; Kadish, K. M. *Inorg. Chem.* **1982**, *21*, 4248.
(34) Chang, D.; Malinski, T.; Ulman, A.; Kadish, K. M. *Inorg. Chem.* **1984**, *23*, 817.
(35) Kadish, K. M.; Boisselier-Cocolios, B.; Simonet, B.; Chang, D.; Ledon, H.; Cocolios, P. *Inorg. Chem.* **1985**, *24*, 2148.
(36) Kadish, K. M.; Morrison, M. *Inorg. Chem.* **1976**, *15*, 980.
(37) Kadish, K. M. *Prog. Inorg. Chem.* **1986**, *34*, 435–605.

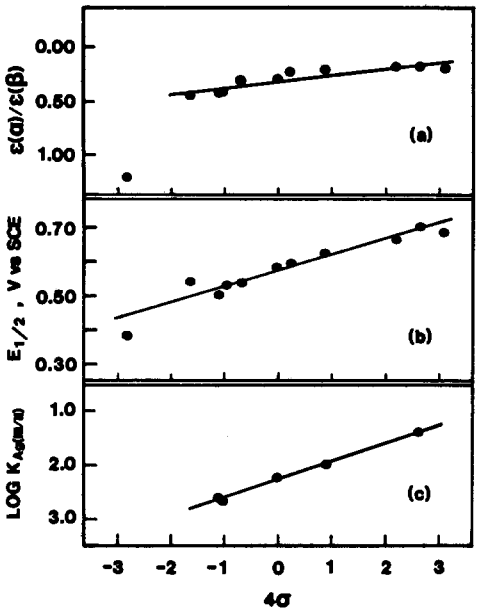

Figure 9. Linear free energy relationships between (a) $\epsilon(\alpha)/\epsilon(\beta)$ and 4σ in Me_2SO, (b) $E_{1/2}$ for reaction 1 and 4σ in Me_2SO, and (c) log $k_{Ag(III/II)}$ for reaction 5 and 4σ in Me_2SO, 0.1 M TBAP.

0.07, 0.05, and 0.07 V for the first oxidation in CH_2Cl_2, Me_2SO, and pyridine and 0.04 or 0.05 V for the first reduction of ((*p*-X)TPP)Ag in all three solvents. In contrast, a ρ = 0.07 V was measured for the second reduction of ((*p*-X)TPP)Ag in pyridine, and this value can be compared to a ρ = 0.05 V for the same reaction in Me_2SO. These latter slopes are given in Figure 8.

The electronic absorption spectra of each ((*p*-X)TPP)Ag^{II} complexes were obtained in Me_2SO, py, and CH_2Cl_2. These spectral data are summarized in Table V. Absorption maxima of the ((*p*-X)TPP)Ag^{II} complexes are blue-shifted compared to spectra of closed d-shell metalloporphyrins and thus are classified as hypso type.[5] The Soret and Q bands of the ((*p*-X)TPP)Ag complexes are almost identical in CH_2Cl_2 and Me_2SO, and only a 2–5-nm shift is seen in py. The spectral shifts in pyridine suggest that axial coordination may occur in this solvent, and this has also been indicated by ESR studies.[22]

Plots of λ_β (in cm^{-1}) vs. the $\epsilon(\alpha)/\epsilon(\beta)$ ratio are linear. This latter ratio is related to the electron density on the porphyrin ring,[38-40] and as expected, a general trend between the $\epsilon(\alpha)/\epsilon(\beta)$ ratio and 4σ is obtained. This plot is shown in Figure 9a. One exception to the general trend is evident for ((*p*-NEt_2)TPP)Ag. This macrocycle is known to have spectral properties quite different from those of other ((*p*-X)TPP)M and ((*p*-X)TPP)MX complexes,[33-35] and it is not surprising that this point does not fit the plot.

The slope of the $E_{1/2}$ vs. 4σ plot is 0.05 V for the oxidation of ((*p*-X)TPP)Ag in Me_2SO. These data are presented in Figure 9b. A plot of log $k_{Ag(III/II)}$ for reaction 5 vs. 4σ is presented in Figure 9c. As seen in this figure, the homogeneous electron-transfer rate constant decreases substantially with an increasing value of the substituent constants given by 4σ. This effect can be related to the fact that the half-wave potentials of the Ag(III)/Ag(II) transition are shifted positively with increasing values of 4σ. The higher the electron-withdrawing ability of the substituent, the more difficult it is to oxidize the complex. A similar correlation between the standard rate constant for homogeneous electron transfer, k_s, and substituent constants for ((*p*-X)TPP)Ag was attempted by Po and Jones,[14] but no effect was observed. This was rationalized on the basis that the porphyrin substituent on ((*p*-X)TPP)Ag was too far removed from the Ag(II) central ion

Table V. UV–Visible Properties (λ, nm ($\epsilon \times 10^{-4}$, cm^{-1} M^{-1})) of the ((*p*-X)TPP)Ag^{II} Complexes in Me_2SO, py, and CH_2Cl_2

	Me_2SO				CH_2Cl_2				py			
porphyrin	Soret	β	α	$\epsilon(\alpha)/\epsilon(\beta)$	Soret	β	α	$\epsilon(\alpha)/\epsilon(\beta)$	Soret	β	α	$\epsilon(\alpha)/\epsilon(\beta)$
((*p*-NO_2)TPP)Ag	428 (24)	540 (1.8)	576 (0.37)	0.20	428 (21)	542 (1.4)	580 (0.25)	0.18	432 (18)	544 (1.4)	578 (0.42)	0.30
((*p*-CN)TPP)Ag	425 (53)	539 (2.9)	574 (0.54)	0.18	425 (47)	540 (2.3)	573 (0.48)	0.21	428 (53)	542 (2.8)	575 (0.60)	0.21
((*p*-CF_3)TPP)Ag	422 (40)	538 (2.0)	572 (0.38)	0.19	423 (37)	538 (1.5)	575 (0.26)	0.18	425 (48)	539 (2.3)	572 (0.41)	0.18
((*p*-Cl)TPP)Ag	424 (60)	538 (2.9)	572 (0.63)	0.22	425 (47)	539 (2.0)	569 (0.43)	0.22	426 (53)	541 (2.4)	575 (0.47)	0.20
((*p*-F)TPP)Ag	422 (25)	538 (1.2)	570 (0.26)	0.22	422 (22)	538 (1.0)	576 (0.21)	0.21	426 (26)	541 (1.3)	571 (0.26)	0.20
(TPP)Ag	422 (24)	538 (1.1)	569 (0.33)	0.30	423 (51)	539 (2.3)	569 (0.44)	0.19	426 (31)	540 (1.6)	573 (0.27)	0.17
((*p*-CH_3)TPP)Ag	422 (29)	540 (1.3)	574 (0.41)	0.32	422 (28)	542 (1.1)	575 (0.32)	0.29	425 (31)	544 (1.3)	578 (0.41)	0.32
((*p*-OC_2H_5)TPP)Ag	432 (29)	545 (1.2)	579 (0.52)	0.43	429 (26)	542 (1.2)	580 (0.48)	0.40	432 (27)	544 (1.4)	582 (0.61)	0.44
((*p*-OCH_3)TPP)Ag	427 (39)	540 (1.9)	577 (0.83)	0.44	427 (47)	542 (2.0)	577 (0.67)	0.34	430 (46)	543 (2.0)	578 (0.78)	0.39
((*p*-$OCH_2C_6H_5$)TPP)Ag	427 (48)	541 (2.2)	577 (1.0)	0.45	428 (37)	542 (1.6)	578 (0.60)	0.38	430 (38)	543 (1.6)	579 (0.62)	0.39
((*p*-NEt_2)TPP)Ag	442 (15)	549 (1.4)	594 (1.7)	1.21	437 (18)	547 (0.96)	588 (0.75)	0.78	443 (13)	550 (0.99)	593 (1.1)	0.11

(38) Meot-Ner, M.; Adler, A. D. *J. Am. Chem. Soc.* **1975**, *97*, 5107.
(39) Shroyer, A. L.; Lonberau, C.; Eaton, S. S. *J. Org. Chem.* **1980**, *45*, 4296.
(40) Gouterman, M.; Schwarz, F. P.; Smith, P. D.; Dolphin, D. *J. Chem. Phys.* **1973**, *59*, 676.

Table VI. UV-Visible Absorbance of $[((p\text{-X})TPP)Ag^{III}]^+$ in Me_2SO, 0.1 M TBAP

porphyrin	λ, nm (ε × 10^{-4}, cm^{-1} M^{-1})		
$[((p\text{-CN})TPP)Ag^{III}]^{+a}$	427 (14.9)	536 (2.0)	
$[((p\text{-Cl})TPP)Ag^{III}]^{+a}$	426 (10.9)	537 (1.8)	
$[(TPP)Ag^{III}]^{+b}$	428 (17)	537 (1.6)	
$[((p\text{-}OC_2H_5)TPP)Ag^{III}]^{+b}$	452 (14)	546 (3.1)	578 (2.0)
$[((p\text{-}OCH_3)TPP)Ag^{III}]^{+a}$	449 (8.8)	543 (2.0)	580 (sh)

[a] Chemically generated with $Ce(SO_4)_2$. [b] Electrochemically generated.

to significantly influence the Ag(II)/Ag(III) reaction.

Table VI shows spectral data for five different $((p\text{-X})TPP)Ag^{III}$ complexes that were chemically or electrochemically generated by oxidation of $((p\text{-X})TPP)Ag^{II}$ in Me_2SO. As seen in this table, the electron-donating groups have the strongest substituent effect on the Ag(III) spectra. Only small shifts of the absorption peaks occur for $[((p\text{-X})TPP)Ag]^+$ where X = CN, Cl, or H. However, a shift of about 20 nm occurs for the Ag(III) complexes that contain porphyrins with X = OCH_3 or OC_2H_5. No explanation for this shift is available at present, but this may be related to the effect of Me_2SO coordination.

In summary, this study has presented the first detailed electrochemical and spectral characterizations of silver porphyrin electrode reactions in nonaqueous media. Eleven different complexes of $((p\text{-X})TPP)Ag$ were investigated in three different solvent systems. It is significant to note that the electrochemically generated Ag(I) porphyrins were sufficiently stable in Me_2SO and py so that they could be spectrally characterized. These complexes could also be further reduced to form the anion radicals without demetalation.

Acknowledgment. The support of the National Science Foundation (Grant No. CHE-8515411) is gratefully acknowledged.

Registry No. $((p\text{-}NO_2)TPP)Ag$, 102682-18-8; $((p\text{-}NO_2)TPP)Ag^+$, 102682-24-6; $((p\text{-}NO_2)TPP)Ag^{2+}$, 102682-29-1; $((p\text{-}NO_2)TPP)Ag^-$, 102682-37-1; $((p\text{-CN})TPP)Ag$, 102682-19-9; $((p\text{-CN})TPP)Ag^+$, 102696-36-6; $((p\text{-CN})TPP)Ag^{2+}$, 102682-30-4; $((p\text{-CN})TPP)Ag^-$, 102682-38-2; $((p\text{-CN})TPP)Ag^{2-}$, 102682-47-3; $((p\text{-}CF_3)TPP)Ag$, 102682-20-2; $((p\text{-}CF_3)TPP)Ag^+$, 102682-25-7; $((p\text{-}CF_3)TPP)Ag^{2+}$, 102682-31-5; $((p\text{-}CF_3)TPP)Ag^-$, 102682-39-3; $((p\text{-Cl})TPP)Ag$, 75964-88-4; $((p\text{-Cl})TPP)Ag^+$, 77761-16-1; $((p\text{-Cl})TPP)Ag^{2+}$, 102682-32-6; $((p\text{-Cl})TPP)Ag^-$, 102682-40-6; $((p\text{-F})TPP)Ag$, 76500-30-6; $((p\text{-F})TPP)Ag^+$, 77701-69-0; $((p\text{-F})TPP)Ag^{2+}$, 102696-37-7; $((p\text{-F})TPP)Ag^-$, 102682-41-7; $(TPP)Ag$, 14641-64-6; $(TPP)Ag^+$, 101567-28-6; $(TPP)Ag^{2+}$, 77701-68-9; $(TPP)Ag^-$, 59980-02-8; $((p\text{-}CH_3)TPP)Ag$, 75964-91-9; $((p\text{-}CH_3)TPP)Ag^+$, 77761-15-0; $((p\text{-}CH_3)TPP)Ag^{2+}$, 102682-33-7; $((p\text{-}CH_3)TPP)Ag^-$, 102682-42-8; $((p\text{-}OC_2H_5)TPP)Ag$, 102682-21-3; $((p\text{-}OC_2H_5)TPP)Ag^+$, 102682-26-8; $((p\text{-}OC_2H_5)TPP)Ag^{2+}$, 102682-34-8; $((p\text{-}OC_2H_5)TPP)Ag^-$, 102682-43-9; $((p\text{-}OCH_3)TPP)Ag$, 75964-92-0; $((p\text{-}OCH_3)TPP)Ag^+$, 77701-66-7; $((p\text{-}OCH_3)TPP)Ag^{2+}$, 102682-35-9; $((p\text{-}OCH_3)TPP)Ag^-$, 102682-44-0; $((p\text{-}OCH_2C_6H_5)TPP)Ag$, 102682-22-4; $((p\text{-}OCH_2C_6H_5)TPP)Ag^+$, 102682-27-9; $((p\text{-}OCH_2C_6H_5)TPP)Ag^{2+}$, 102682-36-0; $((p\text{-}OCH_2C_6H_5)TPP)Ag^-$, 102682-45-1; $((p\text{-}NEt_2)TPP)Ag$, 102682-23-5; $((p\text{-}NEt_2)TPP)Ag^+$, 102682-28-0; $((p\text{-}NEt_2)TPP)Ag^-$, 102682-46-2; Ce, 7440-45-1; hydrazine, 302-01-2.

Contribution from the Department of Chemistry,
The University of Houston—University Park, Houston, Texas 77004

Electrochemistry, Spectroelectrochemistry, and Ligand Addition Reactions of an Easily Reducible Cobalt Porphyrin. Reactions of (Tetracyanotetraphenylporphinato)cobalt(II) ($((CN)_4TPP)Co^{II}$) in Pyridine and in Pyridine/Methylene Chloride Mixtures

X. Q. Lin, B. Boisselier-Cocolios, and K. M. Kadish*

Received April 3, 1986

The electrochemistry, spectroelectrochemistry, and pyridine binding reactions of $((CN)_4TPP)Co^{II}$ were investigated in nine nonaqueous solvents. The four electron-withdrawing CN groups on the porphyrin ring lead to extremely facile reductions such that three one-electron additions could be observed within the range of the solvent. The first reduction occurred between −0.21 and −0.51 V vs. SCE and was assigned as due to formation of Co(II) anion radical. This is in contrast to reduction of unsubstituted $(TPP)Co^{II}$ where the formation of Co(I) is postulated to occur. The second reduction of $((CN)_4TPP)Co$ occurs between −0.80 and −0.94 V vs. SCE and is assigned as due to formation of a Co(I) anion radical. Finally, the third reduction occurs between −1.72 and −1.78 V vs. SCE and is assigned as due to formation of a Co(I) dianion. All three reductions were monitored by thin-layer spectroelectrochemistry, and the spectrum of each reduction product was obtained. A spectrum of electrooxidized $((CN)_4TPP)Co^{II}$ was also obtained in pyridine and methylene chloride. The former solvent is the only one in which a well-defined Co(II) ⇄ Co(III) transition was observed. In addition, the electrochemistry and pyridine binding reactions of $((CN)_4TPP)Co$ were investigated in CH_2Cl_2/pyridine mixtures. Values of $E_{1/2}$ for each electrode reaction were monitored as a function of pyridine concentration, and on the basis of these data, an overall oxidation-reduction and ligand addition scheme was formulated. Stability constants were measured for the stepwise addition of two pyridine molecules to $((CN)_4TPP)Co^{II}$ and $[((CN)_4TPP)Co^{III}]^+$. Similar magnitudes of formation constants were obtained by using electrochemical and spectral methods to monitor the ligand binding reactions of Co(II). Both mono- and bis(pyridine) adducts to Co(II) were identified by electronic absorption spectroscopy.

Introduction

Electrochemical studies of cobalt porphyrins have been the subject of numerous publications.[1-3] Nearly 20 years ago, Stanienda and Biebl[4] first reported potentials for oxidation of several synthetic cobalt(II) porphyrins in nonaqueous media. Three one-electron oxidations were observed. These reactions were later assigned as due to the Co(II)/Co(III) couple followed by the reversible formation of a Co(III) cation radical and a Co(III) dication at more positive potentials.[5-8]

Reductions of Co(II) porphyrins in nonaqueous media have also been studied in great detail.[5,6,9-12] The first electroreduction

(1) Kadish, K. M. *Prog. Inorg. Chem.* **1986**, *34*, 435-605.
(2) Felton, R. H. In *The Porhyrins*; Dolphin, D., Ed.; Academic: New York, 1978; Vol. V, Chapter 3.
(3) Davis, D. G. In *The Porphyrins*; Dolphin, D., Ed.; Academic: New York, 1978; Vol. V, Chapter 4.
(4) Stanienda, A.; Biebl, G. *Z. Phys. Chem. (Munich)* **1967**, *52*, 254.
(5) Walker, F. A.; Beroiz, D.; Kadish, K. M. *J. Am. Chem. Soc.* **1976**, *98*, 3484.
(6) Truxillo, L. A.; Davis, D. G. *Anal. Chem.* **1975**, *47*, 2260.
(7) Wolberg, A. *Isr. J. Chem.* **1974**, *12*, 1031.
(8) Wolberg, A.; Manassen, J. *J. Am. Chem. Soc.* **1970**, *92*, 2982.
(9) Felton, R. H.; Linschitz, M. *J. Am. Chem. Soc.* **1966**, *88*, 1113.
(10) Kadish, K. M.; Davis, D. G. *Ann. N.Y. Acad. Sci.* **1973**, *206*, 495.

0020-1669/86/1325-3242$01.50/0